

## Atomic-Scale Spin Spiral with a Unique Rotational Sense: Mn Monolayer on W(001)

P. Ferriani, <sup>1,\*</sup> K. von Bergmann, <sup>1</sup> E. Y. Vedmedenko, <sup>1</sup> S. Heinze, <sup>1</sup> M. Bode, <sup>1,†</sup> M. Heide, <sup>2</sup> G. Bihlmayer, <sup>2</sup> S. Blügel, <sup>2</sup> and R. Wiesendanger <sup>1</sup>

<sup>1</sup>Institute of Applied Physics, University of Hamburg, Jungiusstrasse 11, 20355 Hamburg, Germany
<sup>2</sup>Institut für Festkörperforschung, Forschungszentrum Jülich, 52425 Jülich, Germany
(Received 15 April 2008; published 7 July 2008)

Using spin-polarized scanning tunneling microscopy we show that the magnetic order of 1 monolayer Mn on W(001) is a spin spiral propagating along  $\langle 110 \rangle$  crystallographic directions. The spiral arises on the atomic scale with a period of about 2.2 nm, equivalent to only 10 atomic rows. *Ab initio* calculations identify the spin spiral as a left-handed cycloid stabilized by the Dzyaloshinskii-Moriya interaction, imposed by spin-orbit coupling, in the presence of softened ferromagnetic exchange coupling. Monte Carlo simulations explain the formation of a nanoscale labyrinth pattern, originating from the coexistence of the two possible rotational domains, that is intrinsic to the system.

DOI: 10.1103/PhysRevLett.101.027201 PACS numbers: 75.70.Ak, 68.37.Ef, 71.15.Mb

Magnetism-based data storage technology relies on the fact that information, i.e., the magnetic state of the area representing the bits, is stable over time. From the microscopic point of view, the direction of the magnetic moments is stabilized mainly by the spin-orbit interaction, which couples the spin to the crystal lattice and is responsible for the occurrence of easy and hard magnetization axes. Based on this picture, the need for nanoscale magnetic devices called scientists to the quest for high magnetic anisotropy materials (see, e.g., Ref. [1]).

However, with decreasing magnetic bit sizes the structural inversion asymmetry of interfaces and surfaces comes into play. A surprising consequence of this fact was recently demonstrated [2], namely, that this symmetry breaking in combination with spin-orbit coupling (SOC) leads to the Dzyaloshinskii-Moriya interaction (DMI) favoring noncollinear magnetic order [3,4]. Although the DMI, because of its relativistic nature, is usually expected to be negligible compared to the nonrelativistic exchange interaction, it is sufficiently strong to impose a nanoscale leftrotating cycloidal spin spiral (SS) on the otherwise antiferromagnetic Mn monolayer on W(110): adjacent moments slightly deviate from the collinear configuration by about 7°, resulting in a long-period SS [2].

Many open issues of this new phenomenon remain. In noncentrosymmetric bulk materials the DMI is the origin of the weak ferromagnetism of parent antiferromagnets [4]. What are the consequences of the DMI in thin films possessing ferromagnetic exchange coupling, e.g., can it destabilize a ferromagnetic state? And what happens to the long-range magnetic order if SS's of different propagation directions are energetically degenerate due to symmetry? Can the DMI modify the magnetic order even on the atomic scale?

As shown in this Letter, 1 ML Mn/W(001) is an ideal system to address these points: As opposed to the antiferromagnetic Mn/W(110), this system exhibits strong ferromagnetic exchange interaction [5] and a fourfold-symmetric square surface lattice. Spin-polarized scanning

tunneling microscopy (SP-STM) measurements reveal a SS, i.e., magnetic moments rotating continuously from one atom to the next, propagating along  $\langle 110 \rangle$  directions with a period of about 2.2 nm, corresponding to only 10 atomic rows. Based on first-principles calculations, we attribute the origin of the SS to the DMI and to the softening of the exchange coupling for configurations close to the ferromagnetic state due to substrate-induced competing ferroand antiferromagnetic interactions. We find that the SS is a left-handed cycloid, i.e., the magnetic moments are confined in a plane parallel to the propagation direction and normal to the surface. Using the Monte Carlo method we simulated large sample areas and found that domains of SS's propagating along symmetry-equivalent crystallographic directions form an intriguing nanoscale labyrinth pattern as also found in experiments.

The SP-STM experiments were performed at T=13 K with an external field B of up to 2.5 T applied perpendicular to the sample surface [6]. The preparation of tips and samples was done *in situ* in ultrahigh vacuum. Tips are made from W wire and flashed to high temperature *in vacuo*; for SP-STM they were then coated with  $\approx 10$  ML of Fe and annealed. Mn was evaporated from a crucible with typical deposition rates of approximately 1 ML per min with the sample held at about 500 K.

Typical spin-resolved measurements of the Mn monolayer on W(001) are shown in Fig. 1. In the constant-current image in Fig. 1(a) individual atoms of the monolayer area are clearly resolved. The white regions correspond to islands of the second atomic layer. The monolayer area is dominated by a stripe pattern along  $\langle 110 \rangle$  directions. By comparison with measurements performed with a non-magnetic tip we can assign this superstructure to the magnetic structure of the sample. The Fe-coated tip used is sensitive to the in-plane component of the magnetization (see inset) and thus atoms imaged bright have a magnetic moment with a large component in one in-plane direction, while for darker atoms the magnetic moment points in the opposite in-plane direction. The periodicity of the mag-

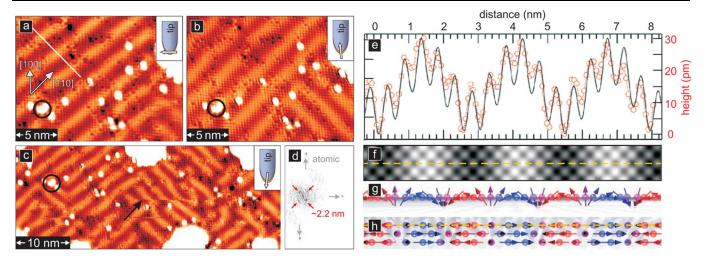


FIG. 1 (color online). Spin-resolved STM measurements of 1 ML Mn/W(001). Constant-current image with magnetic tip sensitive to (a) the in-plane and (b),(c) the out-of-plane component of the sample magnetization (the black circle acts as position marker); (d) Fourier transform of a dI/dU map (not shown) of a sample area with both rotational domains; (e) experimental (circles) and simulated (solid line) profile along the lines indicated in (a) and (f), respectively; (f) simulated SP-STM image, (g) side, and (h) top view of the corresponding model of the SS (colors represent the moment's in-plane component). The following values of bias voltage U and current I were used: (a) and (b) U = -0.1 V, I = 1 nA; (c) U = -0.1 V, I = 0.1 nA.

netic structure can directly be extracted as approximately five diagonals of the square surface unit cell, i.e., about 2.2 nm.

To identify the magnetic state of 1 ML Mn/W(001) we imaged the same sample area with a tip sensitive to the out-of-plane magnetization achieved by applying an external magnetic field of  $B=\pm 2$  T that aligns the tip magnetic moment along its axis [2]. The resulting constant-current image shown in Fig. 1(b) looks very similar to the one measured with the in-plane sensitive tip (a), but now bright and dark atoms represent magnetic moments pointing normal to the surface plane. This observation of both in-plane and out-of-plane magnetic signals with the same periodicity can only be explained by a SS with spiral axis parallel to the surface [2].

On a larger scale we always find a labyrinthlike structure resulting from the two possible rotational domains as shown in (c). The SS state is unstable towards domain wall movements and phase shifts. A comparison between (a) and (b) shows that the border between the two rotational domains has moved, while in the larger view in (c) a jump in the sample magnetization is indicated by the black arrow. This seems to happen spontaneously also without external field and even in the absence of a magnetic tip as it has been observed with nonmagnetic tips imaging the electronic structure changes due to SOC [7]. We attribute this to the fact that the phase of the SS is only weakly pinned by defects or domain boundaries.

Figure 1(d) displays the Fourier transform of a map of differential conductance (dI/dU) of a sample area with both rotational domains, similar to the one in (c). The spots originating from both the atomic periodicity and the magnetic superstructure are clearly resolved. The profile taken along the white line indicated in (a) is shown in (e) together

with a height profile taken from the simulated SP-STM image in (f), based on the spin-polarized Tersoff-Hamann model [8] in the independent orbital approximation [9]. One can clearly see the atomic corrugation of around 15 pm modulated by the magnetic signal with an amplitude of roughly 20 pm. Sketches visualising the SS are displayed in (g) and (h).

Naturally, the question of the origin of the observed magnetic structure arises. A SS can be driven by two mechanisms: competing exchange interactions or DMI. Although the former seems to be supported by the prediction of SS formation in cubic bulk Mn driven by Heisenberg exchange [10], this mechanism could be suppressed here as a strong nearest-neighbor ferromagnetic exchange interaction was predicted for 1 ML Mn/W(001) [5]. Alternatively, SS's may arise from DMI due to inversion asymmetry at surfaces, as recently demonstrated for the Mn monolayer on a W substrate with a different surface orientation than the one investigated here, i.e., (110) [2].

The answer can be given by studying the noncollinear magnetism of 1 MLMn/W(001) based on density-functional theory with and without SOC. The electronic and magnetic structure has been determined in the local density approximation [11], using the full-potential linearized augmented plane wave (FLAPW) method in film geometry as implemented in the FLEUR code [12]. The system was modeled by a pseudomorphic Mn monolayer on a 7-layer W(001) slab with the experimental W lattice constant (3.165 Å), including the structural surface relaxation reported in Ref. [5]. Scalar-relativistic calculations of homogeneous SS's along high-symmetry directions have been performed in the  $p(1 \times 1)$  unit cell [13], exploiting the generalized Bloch theorem. SOC has been treated as a perturbation to the self-consistent potential of SS's based

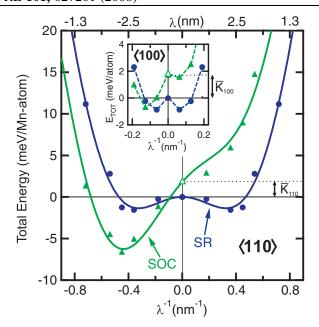


FIG. 2 (color online). Energy of a cycloidal SS propagating along  $\langle 110 \rangle$  (main plot) and  $\langle 100 \rangle$  (inset) as a function of the period length  $|\lambda|$ . The sign of  $\lambda$  indicates the rotational sense. Blue circles and green triangles are results of the scalar-relativistic (SR) and spin-orbit coupling (SOC) calculations, respectively. Solid lines are fits based on the Heisenberg exchange, DMI, and magnetic anisotropy. Fitted curves match data points outside the displayed range up to the Brillouin zone boundary. In the SOC calculation, the zero of the energy corresponds to the ferromagnetic state with moments pointing along the easy axis.

on the magnetic force theorem [14]. SOC is only applied to cycloidal SS's because helical ones, i.e., magnetic moments rotating in a plane orthogonal to the propagation direction, cannot gain energy by DMI due to symmetry arguments [4,14]. 1024 (2500)  $\mathbf{k}_{\parallel}$ -points in the two-dimensional Brillouin zone have been used for the scalar-relativistic (SOC) calculation.

In order to establish whether the formation of noncollinear magnetic order is energetically favorable in 1 ML Mn/W(001), we calculated the energy of homogeneous flat SS's, i.e., magnetic moments confined to a plane and with constant angle between adjacent lattice sites, propagating along (110) crystallographic directions as a function of the period length  $|\lambda|$  (Fig. 2). If we exclude SOC from the calculations, the dispersion is rather flat in a wide interval around the ferromagnetic state, corresponding to  $\lambda^{-1} = 0$ , with a shallow minimum at  $|\lambda| = 3.1$  nm that is only 1.5 meV/Mn atom lower than the ferromagnetic state. As revealed by a fit to the Heisenberg model, in this range the system exhibits strong frustration due to competing ferromagnetic exchange interactions between nearest neighbors and antiferromagnetic exchange interactions beyond nearest neighbors [15]. For smaller  $|\lambda|$ , i.e., for a larger angle between adjacent moments, the energy increases rapidly due to the strong nearest-neighbor ferromagnetic exchange coupling ( $J_1 = 19.7 \text{ meV}$ ) and SS configurations become unfavorable.

The inclusion of SOC introduces two additional energy contributions as seen in Fig. 2. First, the magnetic anisotropy increases the energy of SS's with respect to the ferromagnetic state. While in the latter all moments are parallel to the surface normal, which we determined to be the easy axis, in a SS the majority of the moments deviates from the easy axis. For homogeneous spirals, the resulting energy difference is  $\lambda$ -independent and amounts to the average magnetic anisotropy in the (110) plane, in this case  $\bar{K}_{110} = 1.8$  meV, as can be clearly seen by the vertical shift in the vicinity of  $\lambda^{-1} = 0$ .

The second SOC contribution is the DMI resulting in an odd energy term breaking the symmetry between right-  $(\lambda > 0)$  and left-handed  $(\lambda < 0)$  cycloidal SS's. For the present system, our calculations reveal a nearest-neighbor DMI with coupling constant  $|\mathbf{D}_1| = 4.6$  meV that dominates in the range where the exchange energy is small and leads to a large energy gain of about 6.3 meV/Mn atom for SS states; see Fig. 2. As a result, the ground state is a left-handed cycloidal SS with a period of 2.3 nm, in excellent agreement with the experiments. This period is about 5 times smaller than the 12 nm reported for the SS in 1 ML Mn/W(110) [2] and the angle between adjacent moments is about 36°, cf. Fig. 1(g), showing that the DMI dramatically modifies the magnetic order even on the atomic scale.

The dispersion for SS's propagating along  $\langle 100 \rangle$  reveals an anisotropy and a DMI energy comparable to what was found for  $\langle 110 \rangle$  directions (inset of Fig. 2). However, due to the faster increase of the exchange energy with  $\lambda^{-1}$ , a SS propagating along  $\langle 100 \rangle$  is energetically less favorable and, consistently, is absent in the experiment.

So far we have explained the origin of the observed atomic scale SS state. In the following, we discuss the magnetic structure on the nanometer scale where different domains result in an intriguing labyrinth pattern as shown in Fig. 1(c). In ferromagnetic films, domain formation typically leads to a reduction of the long-ranged dipolar interaction. Since a SS averaged over one period has no net magnetic moment, the dipolar interaction is no energetic driving force for their appearance in the system investigated here. This leaves us with the question whether the coexistence and the size of rotational domains is an entropic effect reflecting the energetic degeneracy of the geometrically equivalent domain pattern or whether it is caused by defects.

To tackle this issue the nanoscale magnetic order was investigated by the Monte Carlo (MC) method, which can simulate complex spin structures on the 50 nm scale [16,17]. We employed a Heisenberg-type model as implemented in Ref. [18], including symmetric exchange up to the 6th nearest neighbor, DMI between nearest neighbors, magnetic anisotropy, and dipolar interaction. The material parameters were obtained from the *ab initio* calculations

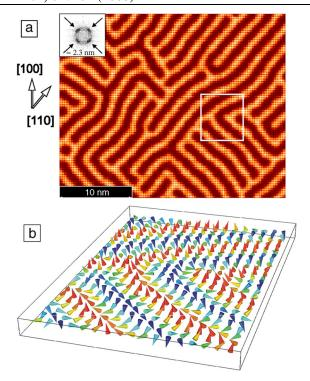


FIG. 3 (color online). (a) Simulated SP-STM image derived from the MC calculations for a Mn monolayer on W(001) at 13 K based on the model of Ref. [9]. The inset shows the corresponding Fourier transform. (b) Perspective view of the area indicated in (a). The spins are represented as cones and the color illustrates their vertical component, ranging from red (up) to dark blue (down).

described above. We used square systems up to  $60 \times 60 \text{ nm}^2$  large with open boundary conditions.

In the following we discuss a typical MC configuration obtained for T = 13 K after slow annealing from a random initial state. The simulated SP-STM image in Fig. 3(a) corresponding to the MC calculation shows a multidomain SS state along  $\langle 110 \rangle$  directions. The periodicity is  $2.3 \pm 0.2$  nm and the whole pattern has a labyrinthine character, similar to the experimental observation in Fig. 1(c). MC simulations allow us to analyze also the internal structure of the spiral, as shown in the perspective view, Fig. 3(b). At T =13 K the SS remains homogeneous within a domain and, in contrast to results from a recent study [19], it shows no significant deviation from being cycloidal. The dipolar coupling (not included in our ab initio calculations) does not modify the results at the atomic scale as it is small (0.5 meV/Mn atom) compared to magnetic anisotropy and DMI.

The moments of Mn atoms in a domain wall deviate from the ideal atomic-scale order causing a domain wall energy of about 0.3 meV/Mn atom for this simulated magnetic state. The energy is clearly positive but smaller than the thermal energy of about 1 meV/Mn atom. Increasing  $|\mathbf{D}_1|/kT$  results in an increase of the domain size and, consequently, a decrease of the total domain wall length in the system (not shown). From this we conclude that the

presence of domains is entropy driven. The low domain wall energy leads to short domain length (5–25 nm) and the labyrinthlike appearance of the whole structure. Interestingly, the SS period is not linear in  $|\mathbf{D}_1|$ , in contrast to what one would expect from a simple micromagnetic model for SS [2]: increasing the DMI by a factor of 2 results in a decrease of  $|\lambda|$  by a factor of 1.2 only. This can be explained by the complex shape of the scalar relativistic dispersion exhibiting strong deviations from a parabolic shape; cf. Fig. 2.

In summary, we establish the DMI as an important mechanism determining the magnetic structure at the atomic scale in thin films. We show for 1 ML Mn/W(001), a system possessing an exchange interaction close to ferromagnetic and high magnetic anisotropy, that the DMI induces a left-handed cycloidal SS with 36° angle between adjacent moments. The DMI, and thereby SOC, turns out to be a potential driving force that destabilizes ferromagnetism in thin films with crucial implications for magnetic nanodevices.

The Stifterverband für die Deutsche Wissenschaft, the Interdisciplinary Nanoscience Center Hamburg, the DFG (SFB 668, BI 823/1-1), the Jülich Supercomputing Centre, and discussions with A. Kubetzka are gratefully acknowledged. E. Y. V. and R. W. acknowledge fruitful discussions with L. Szunyogh and L. Udvardi.

- \*Corresponding author.
- pferrian@physnet.uni-hamburg.de
- <sup>†</sup>Present address: Center for Nanoscale Materials, Argonne National Laboratory, Argonne, IL 60439, USA.
- [1] P. Gambardella et al., Science 300, 1130 (2003).
- [2] M. Bode et al., Nature (London) 447, 190 (2007).
- [3] I. E. Dzialoshinskii, Sov. Phys. JETP 5, 1259 (1957).
- [4] T. Moriya, Phys. Rev. 120, 91 (1960).
- [5] P. Ferriani et al., Phys. Rev. B 72, 024452 (2005).
- [6] O. Pietzsch et al., Rev. Sci. Instrum. 71, 424 (2000).
- [7] M. Bode et al., Phys. Rev. Lett. 89, 237205 (2002).
- [8] D. Wortmann et al., Phys. Rev. Lett. 86, 4132 (2001).
- [9] S. Heinze, Appl. Phys. A 85, 407 (2006).
- [10] J. Hafner and D. Spišák, Phys. Rev. B 72, 144420 (2005).
- [11] H. Vosko, L. Wilk, and M. Nusair, Can. J. Phys. 58, 1200 (1980).
- [12] http://www.flapw.de.
- [13] Ph. Kurz et al., Phys. Rev. B 69, 024415 (2004).
- [14] M. Heide *et al.*, Psi-k Newsletter 78, www.psi-k.org (2006); M. Heide, Ph.D. thesis, RWTH-Aachen, 2006.
- [15] In order to fit the scalar-relativistic data, it was necessary to include exchange interactions at least up to the 5th neighbor in the Heisenberg model, with the following results given in sequence of increasing neighbor distance:  $J_1, \ldots, J_6 = 19.7, -2.5, -1.5, -0.5, -1.4, 0.0 \text{ meV}.$
- [16] M. Bode et al., Nat. Mater. 5, 477 (2006).
- [17] E. Y. Vedmedenko, Phys. Status Solidi B **244**, 1133 (2007).
- [18] E. Y. Vedmedenko et al., Phys. Rev. B 75, 104431 (2007).
- [19] L. Udvardi et al., Physica (Amsterdam) 403B, 402 (2008).